The University of Sydney

School of Civil Engineering
Sydney NSW 2006
AUSTRALIA

http://www.civil.usyd.edu.au/

Centre for Advanced Structural Engineering

Lateral Buckling of Monorail Beams

Research Report No R883

N S Trahair BSc BE MEngSc PhD DEng

August 2007

The University of Sydney

School of Civil Engineering
Centre for Advanced Structural Engineering
http://www.civil.usyd.edu.au/

Lateral Buckling of Monorail Beams

Research Report No R883

N S Trahair BSc BE MEngSc PhD DEng
August 2007

Abstract:

The resistances of steel I-section monorail beams to lateral buckling are difficult to assess because monorails are often not well restrained against twisting. Monorails are supported at intervals along the top flange, but are free along the bottom flange, except at supported ends where vertical stiffeners may restrain the bottom flange. The buckling resistance is increased by the loading which generally acts below the bottom flange and induces restraining torques, but it is not common to take advantage of this. The buckling resistance may also be increased by any restraints against lateral deflection and longitudinal rotation of the top flange at internal supports, but it is difficult to quantify their effects without analyzing the distortion of the monorail web. This paper analyses the influence of restraints on the elastic lateral buckling (without distortion) of monorails loaded at the bottom flange, and shows how this might be accounted for in design.

Keywords: beams, bending, buckling, design, elasticity, member resistance, moments, monorails, steel, torsion.

Copyright Notice

Lateral Buckling of Monorail Beams

N.Trahair@civil.usyd.edu.au

Published by:
School of Civil Engineering
The University of Sydney
Sydney NSW 2006
AUSTRALIA

August 2007

http://www.civil.usyd.edu.au

INTRODUCTION

The resistances of steel I-section monorail beams (Fig. 1) to lateral and lateral-distortional buckling (Fig. 2c and d) are difficult to assess because monorails are often not well restrained against twisting. The bottom flange of a monorail provides a track for the movement of a trolley which carries a hoist. The monorail is supported at intervals along the top flange, but is free along the bottom flange, except at the supported ends where vertical stiffeners may be provided to limit the travel of the trolley and to restrain the bottom flange, as shown in Fig. 2a. At these ends, the restraints are usually effective in preventing lateral deflection u and twist rotation ϕ, as is generally assumed for the prediction of the lateral buckling resistance (Trahair, 1993), but these restraints may be far apart, and the buckling resistance based solely on them may be very low. On the other hand, the buckling resistance is increased by the loading which generally acts below the bottom flange (SA, 2001; Woolcock et al, 2003) and induces restraining torques, but it is not common to take advantage of this.

The buckling resistance may also be increased by any restraints against lateral deflection and longitudinal rotation of the top flange at internal supports, but it is difficult to quantify their effects. The increased resistance caused by longitudinal rotation restraints is accompanied by distortion of the cross-section, in which the bottom flange undergoes differential flange rotations ϕ_B, as shown in Fig. 2b. Distortion is not accounted for in lateral buckling analyses, even though some small distortions may occur as shown in Fig. 2c. Instead, it is assumed that the flange rotations are equal, as shown in Fig. 2d.

A number of common monorail arrangements are shown in Fig. 3. The scope of this paper is limited to the influence of restraints on the elastic lateral buckling of these monorails loaded at the bottom flange, and the consideration of how this might be accounted for in design. The lateral-distortional buckling of monorails is only considered qualitatively, because accurate quantitative analysis requires the analysis of distortion, which is beyond the scope of this paper.

MONORAIL RESTRAINTS

The connections of a monorail to its supports may provide a number of different types of restraint against buckling. The connections to the top flange are normally effective in preventing lateral deflection u_T of the top flange. They usually provide elastic restraints against longitudinal rotation ϕ_T of the top flange, which may sometimes be assumed to be effectively rigid. They may also provide elastic restraints against lateral rotation $\mathrm{d}u_T/\mathrm{d}z$ of the top flange, but these are usually (and conservatively) assumed to be ineffective.

The torsional restraint conditions at a beam section have been classified as fully restrained, partially restrained, or unrestrained (SA, 1998). The ends of monorail beams may be classified as fully restrained torsionally if the lateral deflections of both flanges are prevented (u_T = u_B = 0) , as is the case when lateral deflection u_T and longitudinal rotation ϕ_T of the top flange can be assumed to be prevented and there is a transverse web stiffener which prevents local distortion of the web, as shown in Fig. 2a.

Monorail beams may be considered to be partially restrained against torsion at intermediate supports where lateral deflection u_T and longitudinal rotation ϕ_T of the top flange can be assumed to be prevented, but the bottom flange is unrestrained, as shown in Fig. 2b. The effects of partial torsional restraints on buckling cannot be determined quantitatively unless the effects of distortion are included in the buckling analysis.

Monorail beams should be considered to be unrestrained against torsion wherever longitudinal rotation of the top flange is not prevented, as in Fig. 2c and 2d.

ELASTIC LATERAL BUCKLING OF MONORAILS

The ability of a doubly symmetric I-section monorail to resist elastic lateral buckling depends on its geometry, loading and restraints. The elastic buckling of the monorails shown in Fig. 3 has been analysed using a finite element lateral buckling program FTBER which was developed by extending the theory summarized in Trahair (1993) and used in the computer program PRFELB (Papangelis et al, 1998) to account for eccentric rigid restraints, as described in Trahair and Rasmussen (2005). The results of these analyses for monorails with bottom flange loading are discussed in the following sections.

MONORAIL BEAMS

Single Span Monorails

A simply supported monorail beam which is prevented from deflecting u and twisting ϕ at its supports is shown in Fig. 3a(b1). The maximum moment M_{cr} = QL/4 at elastic lateral buckling of the monorail with a central concentrated load Q which acts at a distance y_Q below the shear centre axis may be closely approximated by using (Trahair, 1993)

$$\frac{M_{cr}}{M_{yz}} = \alpha_m \left\{ \sqrt{\left[1 + \left(\frac{0.4\alpha_m y_Q}{M_{yz}/P_y} \right)^2 \right]} + \frac{0.4\alpha_m y_Q}{M_{yz}/P_y} \right\} \tag{1}$$

in which

$$M_{yz} = \sqrt{\left(\pi^2 EI_y / L^2\right)} \sqrt{\left(GJ + \pi^2 EI_w / L^2\right)} \tag{2}$$

is the elastic lateral buckling moment of a simply supported beam with equal and opposite end moments (Timoshenko and Gere, 1961; Trahair, 1993), in which EI_y is the minor axis flexural rigidity, GJ is the torsional rigidity, EI_w is the warping rigidity, and L is the beam length,

$$P_y = \pi^2 EI_y / L^2 \tag{3}$$

and the moment modification factor α_m which allows for the bending moment distribution is approximated by (SA, 1998)

$$\alpha_m = \frac{1.7M_{max}}{\sqrt{\left(M_2^2 + M_3^2 + M_4^2\right)}} \tag{4}$$

in which M_{max} is the maximum moment and M_2, M_3, and M_4 are the moments at the quarter-, mid-, and three quarter-points. For a central concentrated load, α_m = 1.35.

For monorail beams loaded at the bottom flange, a simpler approximation is given by

$$\frac{M_{cr}L}{\sqrt{EI_yGJ}} = 4 + 4.53K + 0.53K^2 \tag{5}$$

in which

$$K = \sqrt{\frac{\pi^2 EI_w}{GJL^2}} \tag{6}$$

as shown in Fig. 4.

The monorail beam shown in Fig. 3a(b2) has lateral restraints only at the top flange ends, and therefore has no apparent torsional restraint. While it is unlikely that such a monorail would ever be used in practice, it nevertheless has theoretical interest because it is able to resist lateral buckling. This is because the combination of the top flange reactions with the bottom flange load induces restoring torques which resist twist rotation and prevent lateral deflection of the load point. A similar effect stabilizes an unrestrained lifting beam which supports loads from its bottom flange but which itself is supported from its top flange or above (Dux and Kitipornchai, 1990; Trahair, 1993).

The dimensionless elastic buckling loads of these monorail beams may be approximated by using

$$\frac{M_{cr}L}{\sqrt{EI_yGJ}} = 6.5K - 0.13K^2 \tag{7}$$

The solutions of this are significantly lower than those given by Equation 6 for bottom flange loading of beams with full torsional restraints, as shown in Fig. 4.

Also shown in Fig. 4 are the intermediate solutions given by

$$\frac{M_{cr}L}{\sqrt{EI_yGJ}} = 2.6 + 4.5K + 0.44K^2 \tag{8}$$

for monorail beams prevented from deflecting and twisting at one end but with only a top flange lateral restraint at the other (Fig. 3a(b3)).

Two Span Monorails

The monorail beam shown in Fig. 3a(b4) has two equal spans and a single bottom flange load. The variations of the dimensionless elastic buckling load $M_{cr}L/\sqrt{(EI_yGJ)}$ with the load position parameter α are shown in Fig. 5. Also shown are the approximations given by

$$\frac{M_{cr}L}{\sqrt{EI_yGJ}} = (5.5 + 3.3K + 0.69K^2) + \alpha(-10 + 11.7K - 1.2K^2) + \alpha^2(8.5 - 7.2K + 0.9K^2) \quad (9)$$

which are in close agreement.

The monorail beam shown in Fig. 3a(b5) has two unequal spans and a single bottom flange load. The variations of the dimensionless elastic buckling load $M_{cr}L/\sqrt{(EI_yGJ)}$ with the span ratio α are shown in Fig. 6. Also shown are the approximations given by

$$\frac{M_{cr}L}{\sqrt{EI_yGJ}} = (3.5 + 8.6K + 0.74K^2) - (1.9\alpha - 0.31\alpha^2)(0.2 + K + 0.21K^2) \quad (10)$$

which are in close agreement.

MONORAIL CANTILEVERS AND OVERHANGS

Cantilevered Monorail

A cantilevered monorail whose lateral deflection u, rotation $\mathrm{d}u/\mathrm{d}z$, twist rotation ϕ, and warping $\mathrm{d}\phi/\mathrm{d}z$ are prevented at the support and free at the other end is shown in Fig. 3b(c1). The maximum moment M_{cr} = QL caused by an end concentrated load Q which acts at a distance y_Q below the shear centre axis at elastic lateral buckling may be approximated by using (Trahair, 1993)

$$\frac{M_{cr}L}{\sqrt{EI_yGJ}} = 11\left\{1 + \frac{1.2\varepsilon}{\sqrt{1 + 1.2^2\varepsilon^2}}\right\} + 4(K - 2)\left\{1 + \frac{1.2(\varepsilon - 0.1)}{\sqrt{1 + 1.2^2(\varepsilon - 0.1)^2}}\right\} \quad (11)$$

in which

$$\varepsilon = \frac{y_Q}{L}\sqrt{\left(\frac{EI_y}{GJ}\right)} \quad (12)$$

For cantilevers loaded at the bottom flange, a simpler approximation is given by

$$\frac{M_{cr}L}{\sqrt{EI_yGJ}} = 4 + 5.93K + 0.58K^2 \quad (13)$$

as shown in Fig. 7.

Overhanging Monorail

An overhanging monorail (Trahair, 1983) is shown in Fig. 3b(c2). This is similar to the cantilever shown in Fig. 3b(c1), except that there is no warping restraint at the support. The maximum moment M_{cr} = QL caused by an end concentrated load Q which acts at a distance y_Q below the shear centre axis at elastic lateral buckling may be approximated by using (Trahair, 1993)

$$\frac{M_{cr}L}{\sqrt{EI_yGJ}} = 6\left\{1+\frac{1.5(\varepsilon-0.1)}{\sqrt{1+1.5^2(\varepsilon-0.1)^2}}\right\}+1.5(K-2)\left\{1+\frac{3(\varepsilon-0.3)}{\sqrt{1+3^2(\varepsilon-0.3)^2}}\right\} \qquad (14)$$

For overhanging monorails loaded at the bottom flange, a simpler approximation is given by

$$\frac{M_{cr}L}{\sqrt{EI_yGJ}} = 4+2.07K+0.42K^2 \qquad (15)$$

as shown in Fig. 7.

Single Span Monorail with Single Overhang

A monorail with a supported span and an overhang is shown in Fig. 3b(c3). The supported span is prevented from deflecting (u = 0) and twisting (ϕ = 0) at one end and its top flange is prevented from deflecting (u_T = 0) but is free to twist ($\phi_T \neq 0$) at the other support. The variations of the dimensionless elastic buckling moment with the length ratio α and the torsion parameter *K* may be approximated by

$$\frac{M_{cr}L}{\sqrt{EI_yGJ}} = (2.4+1.81K+0.33K^2)-(2.8\alpha-0.6\alpha^2)(0.5+0.38K+0.1K^2) \qquad (16)$$

and are shown in Fig. 8.

These dimensionless buckling moments are significantly less than those given by Equation 15 for the overhanging monorail of Fig. 3b(c2) (see Fig. 7) because the interior support does not prevent twist rotation. Substantial increases in the buckling moment may occur if twist rotation is elastically restrained at this support, but the determination of these increases requires an analysis which accounts for distortion, which is beyond the scope of this paper.

Single Span Monorail with Double Overhang

The double overhanging monorail beam shown in Fig. 3b(c4) has lateral restraints only at the two (interior) supports, and therefore has no apparent torsional restraint. While it is unlikely that such a monorail would ever be used in practice, it nevertheless has theoretical interest because it is able to resist lateral buckling, (as does the monorail beam shown in Fig. 3a(b2) and discussed earlier). This resistance arises from the bottom flange loads, which will exert restoring torques if the beam twists. For equilibrium, the resultant of these loads must act through a point midway between the two supports, as is the case when neither load displaces laterally.

The variations of the dimensionless elastic buckling moments with the length ratio α and the torsion parameter *K* may be approximated by

$$\frac{M_{cr}L}{\sqrt{EI_y GJ}} = (1.28K - 0.062K^2) - (2.42\alpha - 0.47\alpha^2)(0.28K - 0.009K^2) \qquad (17)$$

and are shown in Fig. 9.

DESIGN AGAINST LATERAL BUCKLING

Although design codes generally (AISC, 2005; BSI, 2000; BSI, 2005) have rules for designing beams against lateral buckling, very few have rules which allow the economical design of monorails which are loaded at or below the bottom flange. The Australian code AS4100 (SA, 1998) has a general method of design by buckling analysis which allows the direct use of the results of elastic buckling analyses such as those performed for this paper. For this, the elastic buckling moment M_{cr} is used in the equation

$$\frac{M_{bx}}{M_{sx}} = 0.6\alpha_m \left\{ \sqrt{\left[\left(\frac{\alpha_m M_{sx}}{M_{cr}} \right)^2 + 3 \right]} - \left(\frac{\alpha_m M_{sx}}{M_{cr}} \right) \right\} \le 1 \qquad (18)$$

to determine the nominal major axis moment resistance M_{bx}, in which M_{sx} is the nominal major axis section capacity (reduced below the full plastic moment M_{px} if necessary to allow for local buckling effects), and α_m is a moment modification factor which allows for the non-uniform distribution of bending moment along the beam. The variations of the dimensionless nominal resistance M_{bx} / M_{sx} with the modified slenderness $\sqrt{(M_{sx} / M_{cr})}$ and the moment modification factor α_m are shown in Fig. 10.

While AS4100 provides an approximate method for calculating α_m through Equation 4, this is often conservative and sometimes erratic. Because of this, a more accurate procedure is given in which α_m is calculated from

$$\alpha_m = M_{crs} / M_{yz} \tag{19}$$

in which M_{crs} is the elastic buckling moment of the beam length between points of full lateral and torsional restraint which is unrestrained against lateral rotation and loaded at the shear centre, and M_{yz} is the elastic buckling moment of the same beam under uniform bending (see Equation 2). For cantilevers and overhangs,

$$\alpha_m = 1 \tag{20}$$

When this method is applied to the monorails in Fig. 3, it is found that the values of α_m increase slowly with K, and that conservative approximations can be obtained by using

α_m = 1.35 for the single span beams of Fig. 3a(b1,2,3), (21a)

α_m = 1.0 for the cantilevers and overhangs of Fig. 3b, (21b)

$\alpha_m = 3.32 - 4\,\alpha + 4\,\alpha^2 - 2\,\alpha^3$ for the two span beam of Fig. 3a(b4), (21c)

and $\alpha_m = 1.28 + 0.78\,\alpha$ for the two span beam of Fig. 3a(b5). (21d)

The variations of α_m with α given by Equations 21c and d are shown in Fig. 11.

WORKED EXAMPLE

Problem

Determine the nominal load resistance of the two span monorail of Fig. 3a(b4) for L= 10.0 m, α = 0.5, and the properties shown in Fig. 12.

Solution

A summary of the solution is as follows.

(1) Using Equation 6, K = 0.491
(2) Using Equation 9, M_{cr} = 155.6 kNm.
(3) Using Equation 21c, α_m = 2.07
(4) Using Equation 18, M_{bx} = 134.1 kNm.
(5) Using M_{max}/QL = 0.203, Q = 66.1 kN.

If these calculations are repeated for different values of α, the corresponding values of Q shown in Fig. 12 are obtained. These indicate that the minimum value of Q is approximately equal to 64 kN.

CONCLUSIONS

This paper considers the lateral buckling resistances of steel I-section monorail beams, which are difficult to assess because monorails are often not well restrained against twisting. The resistances are increased by the loading which generally acts below the bottom flange and induces restraining torques, but it is not common to take advantage of this. The resistances may also be increased by any restraints against lateral deflection and longitudinal rotation of the top flanges at internal supports, but it is difficult to quantify these effects without analyzing web distortions.

The scope of the paper is limited to the influence of restraints on the elastic lateral buckling of these monorails loaded at the bottom flange, and the consideration of how this might be accounted for in design. The lateral-distortional buckling of monorails is only considered qualitatively, because accurate quantitative analysis requires the consideration of web distortion.

The paper develops a rational, consistent, and economical design method for determining the nominal lateral buckling resistances of a number of monorail beams, cantilevers and overhangs which are loaded at the bottom flange and supported at the top flange. This method will be conservative for monorails loaded below the bottom flange.

A finite element computer program FTBER is used to analyse the elastic buckling of monorails and simple closed form approximations are presented. These may be used in the method of design by buckling analysis of the Australian code AS4100 (SA, 1998) to determine their nominal moment resistances. This method may be adapted for use with other design codes. A worked example is given of the application of the method.

APPENDIX 1 REFERENCES

AISC (2005), *Specification for Structural Steel Buildings*, American Institute of Steel Construction, Chicago.

BSI (2000), *BS5950 Structural Use of Steelwork in Building. Part 1:2000. Code of Practice for Design in Simple and Continuous Construction: Hot Rolled Sections,* British Standards Institution, London.

BSI (2005), *Eurocode 3: Design of Steel Structures,* British Standards Institution, London.

Dux, PF and Kitipornchai, S (1990), 'Buckling of suspended I-beams', *Journal of Structural Engineering,* ASCE, 116 (7), 1877-91.

Papangelis, JP, Trahair, NS, and Hancock, GJ (1997), *PRFELB – Finite Element Flexural-Torsional Buckling Analysis of Plane Frames,* Centre for Advanced Structural Engineering, University of Sydney.

Papangelis, JP, Trahair, NS, and Hancock, GJ (1998), 'Elastic flexural-torsional buckling of structures by computer', *Computers and Structures*, 68, 125 - 37.

SA (1998), *AS 4100-1998 Steel Structures,* Standards Australia, Sydney.

SA (2001), *AS 1418.18 – Crane Runway and Monorails,* Standards Australia, Sydney.

Trahair, NS (1993), *Flexural-Torsional Buckling of Structures*, E & FN Spon, London.

Trahair, NS and Rasmussen, KJR (2005), 'Flexural-torsional buckling of columns with oblique eccentric restraints', *Journal of Structural Engineering*, ASCE, 131 (11), 1731-7.

Woolcock, ST, Kitipornchai, S, and Bradford, MA (2003), *Design of Portal Frame Buildings*, 3rd edition, Australian Steel Institute, North Sydney.

APPENDIX 2 NOTATION

E	Young's modulus of elasticity
G	shear modulus of elasticity
I_w	warping section constant
I_y	second moment of area about the y principal axis
J	torsion section constant
K	torsion parameter (Equation 6)
L	span length
M_{bx}	lateral buckling moment resistance
M_{cr}	elastic lateral buckling moment
M_{crs}	elastic lateral buckling moment of a beam length between points of full restraint and loaded at the shear centre
M_{max}	maximum moment
M_{px}	fully plastic moment
M_{sx}	section moment capacity
M_{yz}	uniform bending elastic lateral buckling moment
$M_{2,3,4}$	moments at quarter-, mid-, and three-quarter-points
P_y	minor axis column buckling load (Equation 3)
Q	concentrated load
u	shear centre deflection parallel to the x principal axis
u_B, u_T	bottom and top flange deflections
x, y	principal axes
y_Q	distance of load point below centroid
z	distance along beam
α	length ratio
α_m	moment modification factor
ε	load height parameter (Equation 12)
ϕ	angle of twist rotation
ϕ_B , ϕ_T	bottom and top flange twist rotations

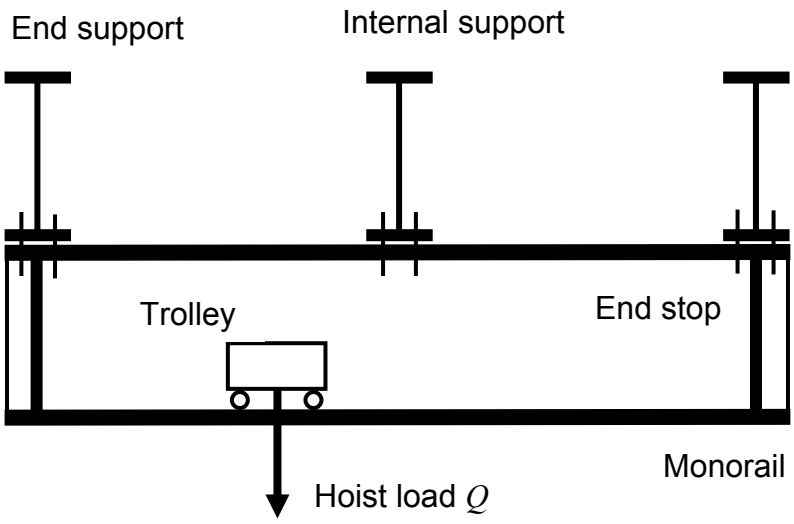

Fig. 1 Single span monorail

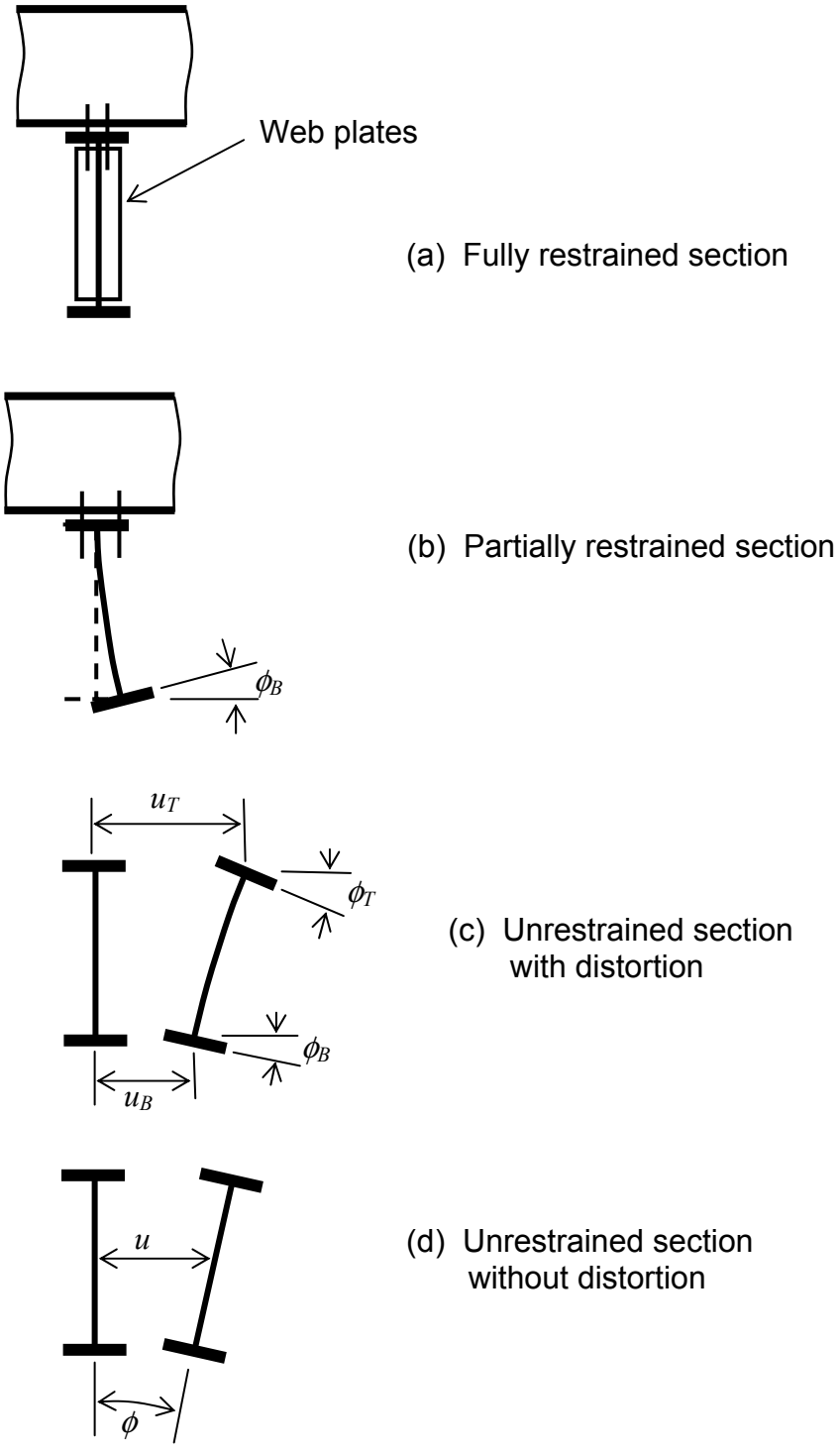

Fig. 2 Cross-section deformations of monorails

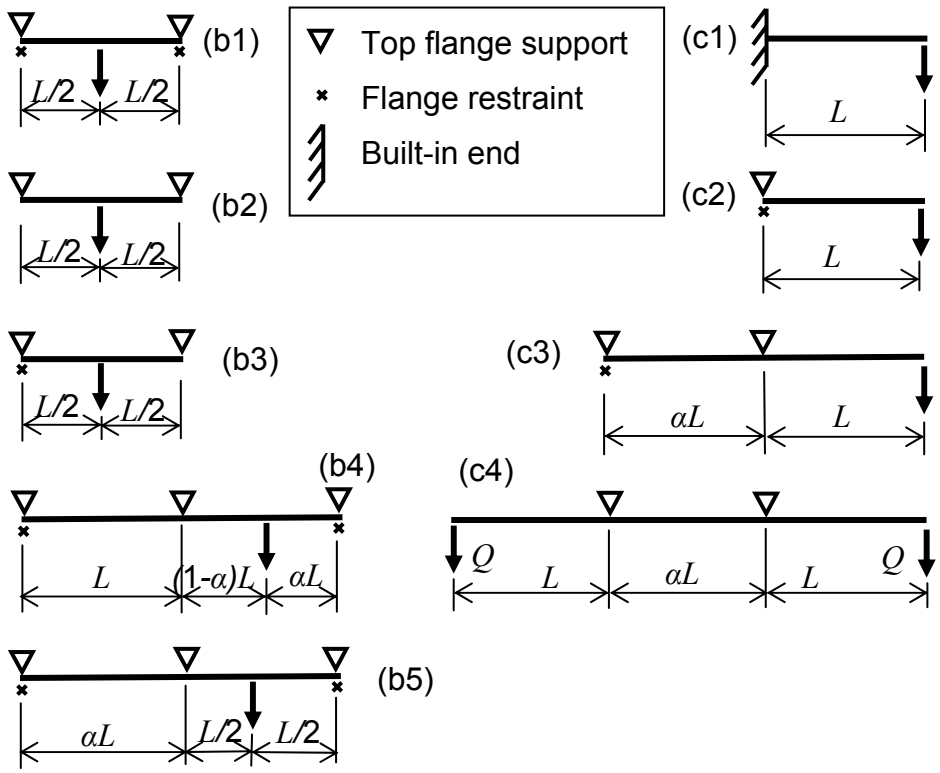

Fig. 3 Monorail beams and cantilevers

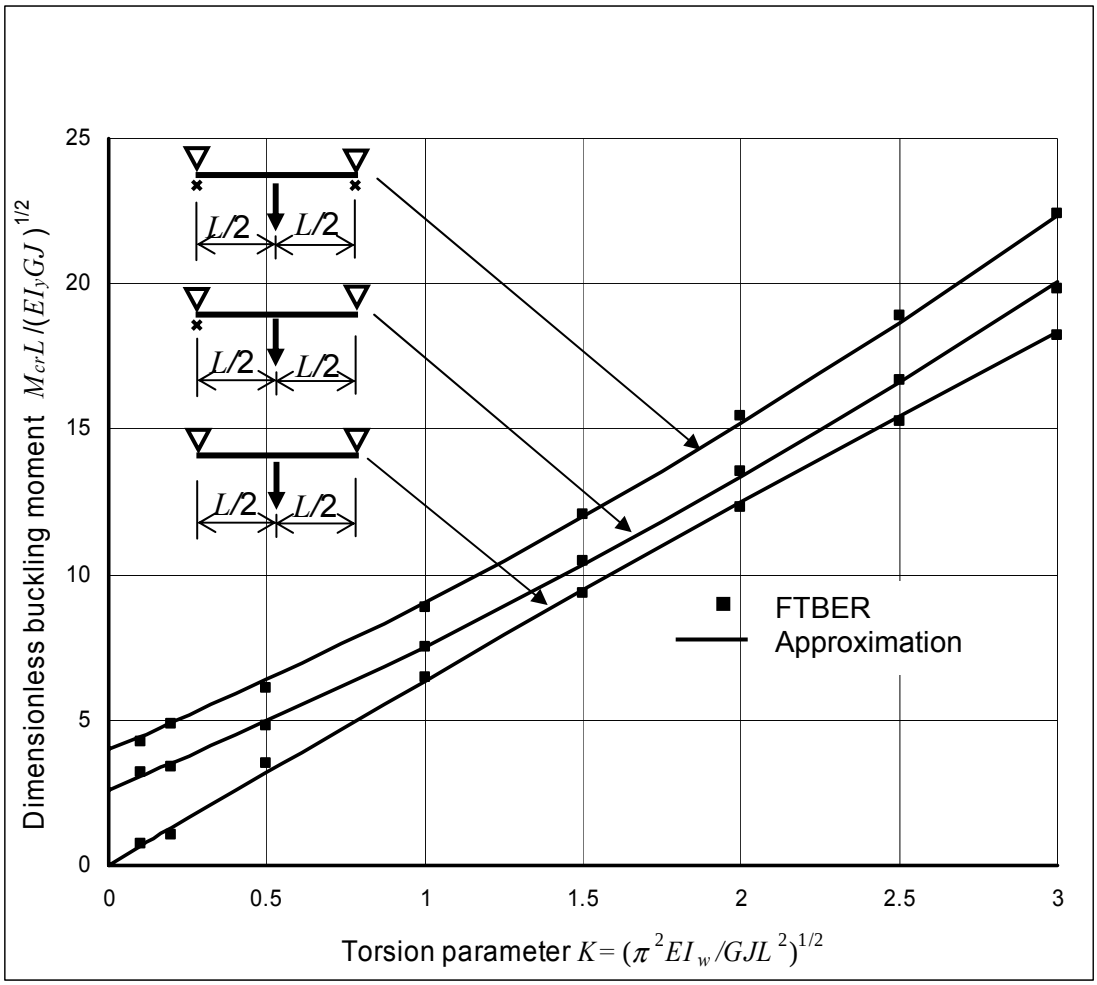

Fig. 4 Single span monorail beams

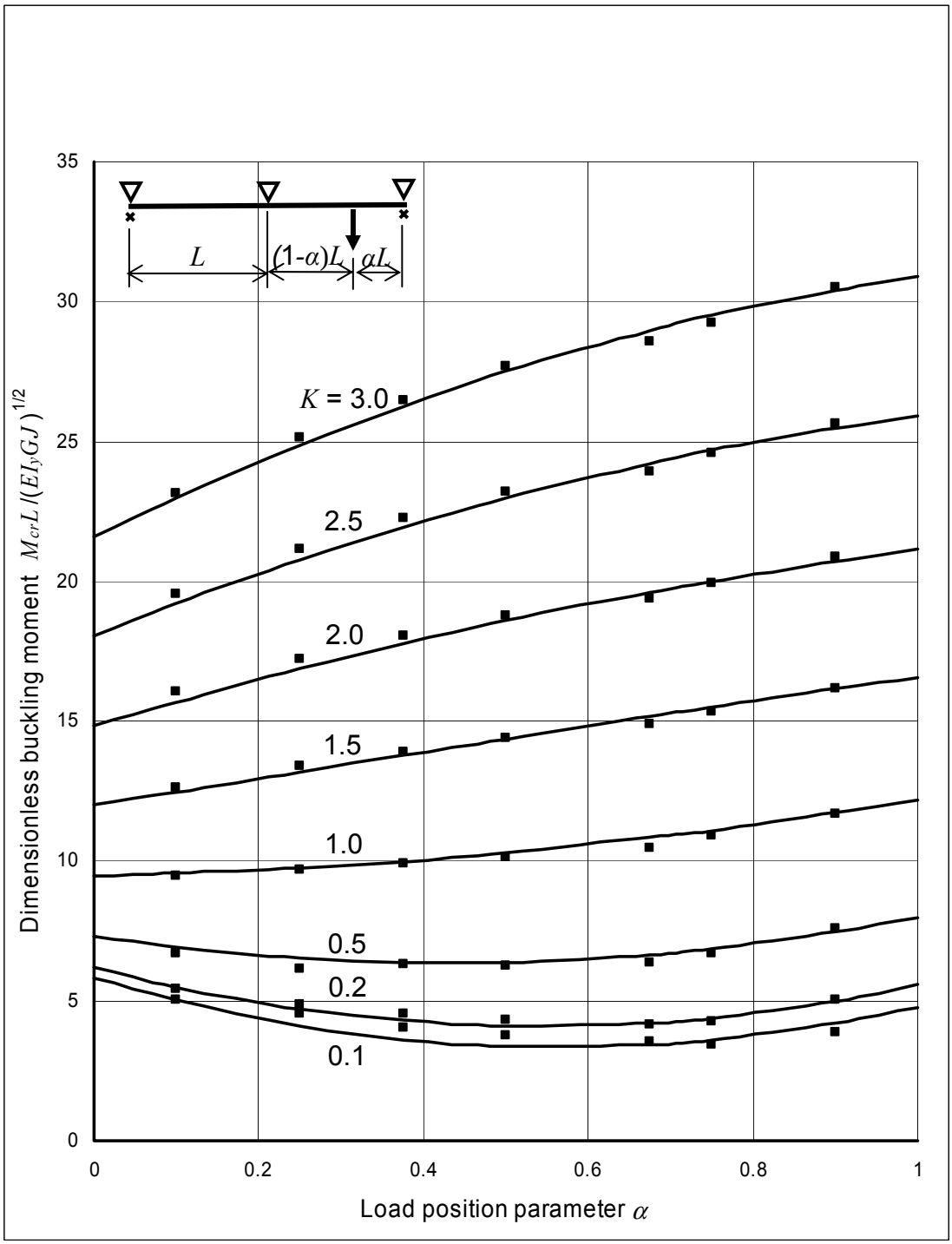

Fig. 5 Effect of load position for two span monorails

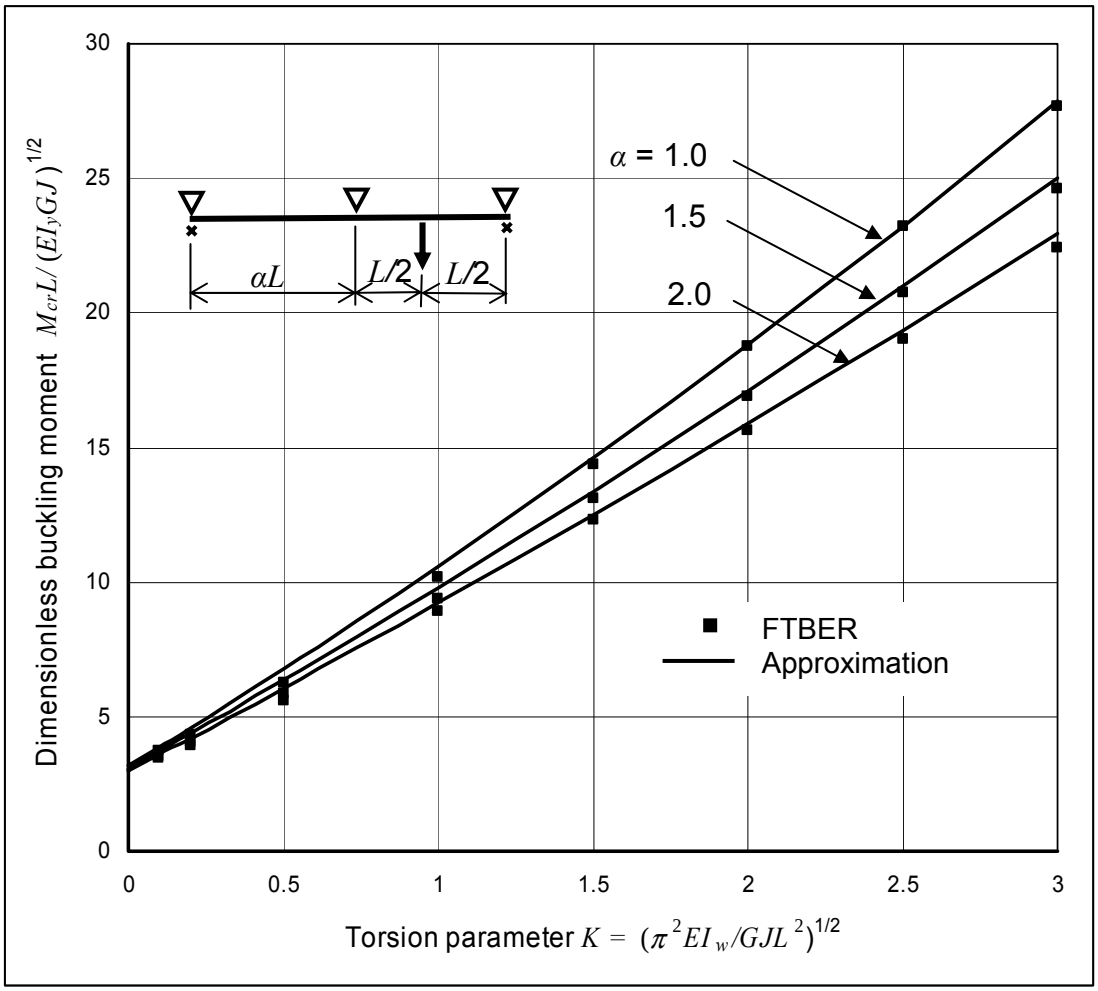

Fig. 6 Effect of span ratio for two span monorails

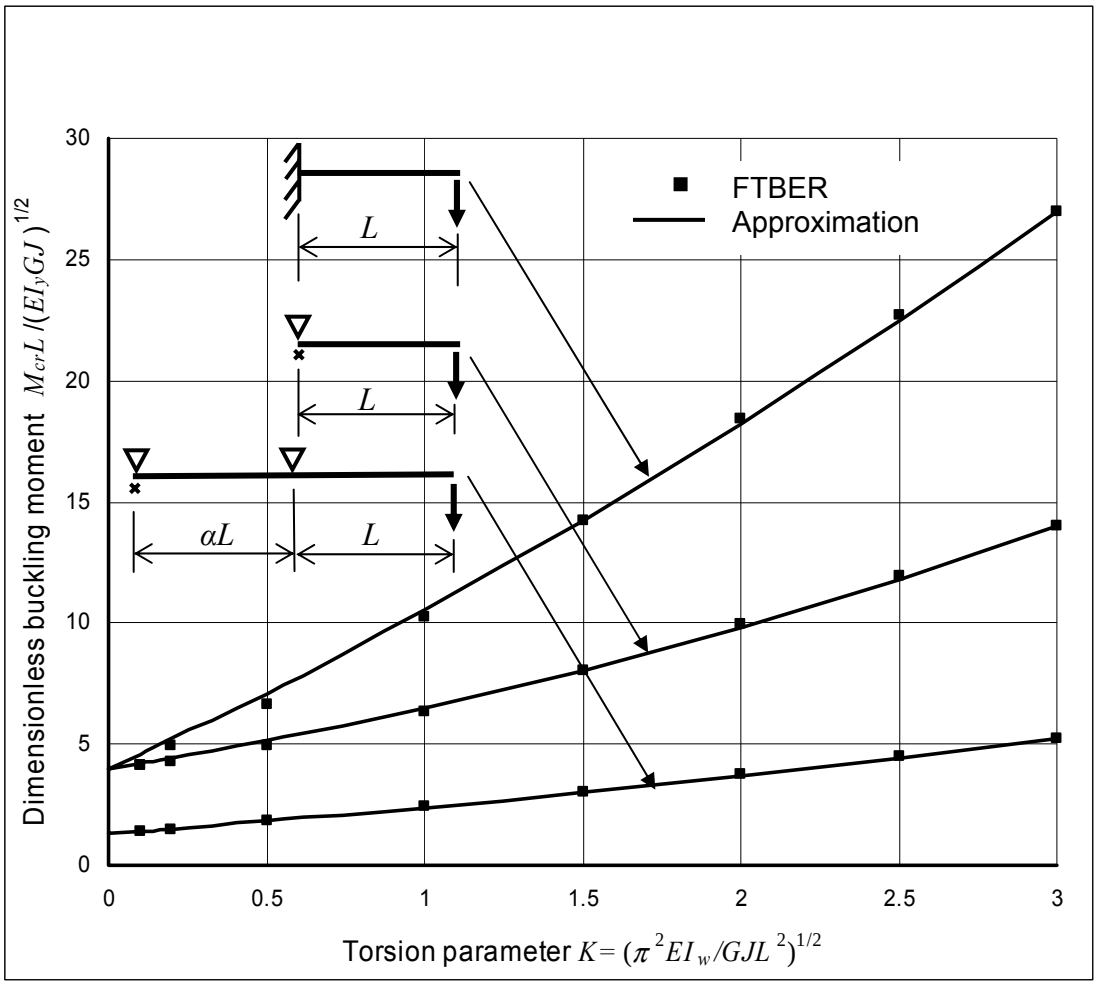

Fig. 7 Cantilever and overhanging monorails

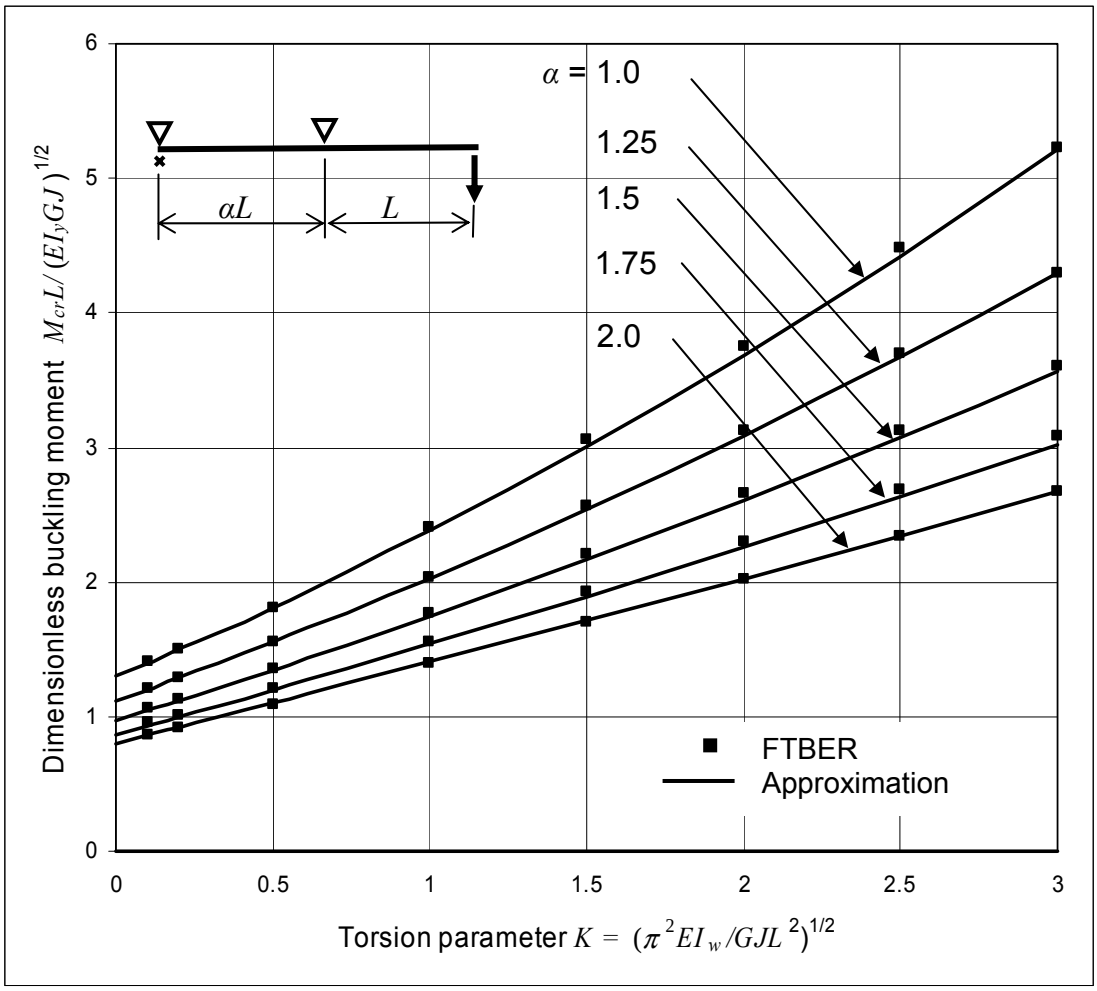

Fig. 8 Single span monorail with overhang

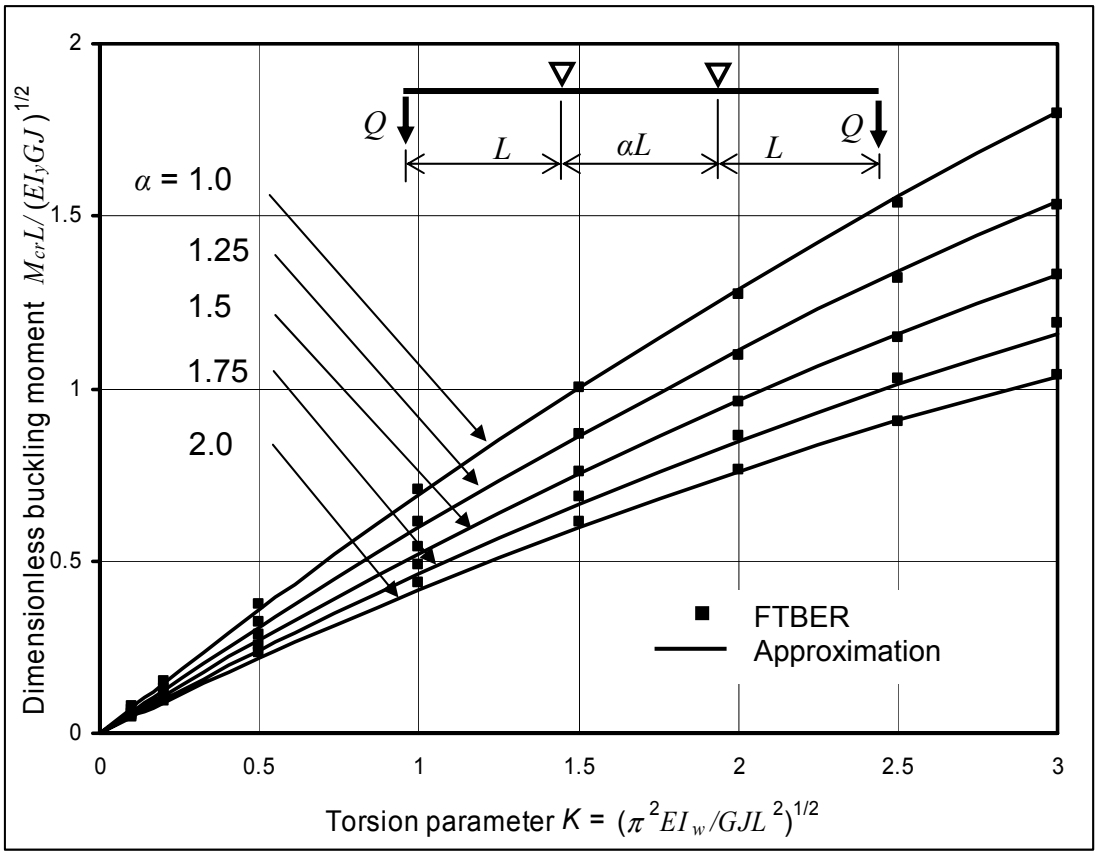

Fig. 9 Single span monorail with double overhang

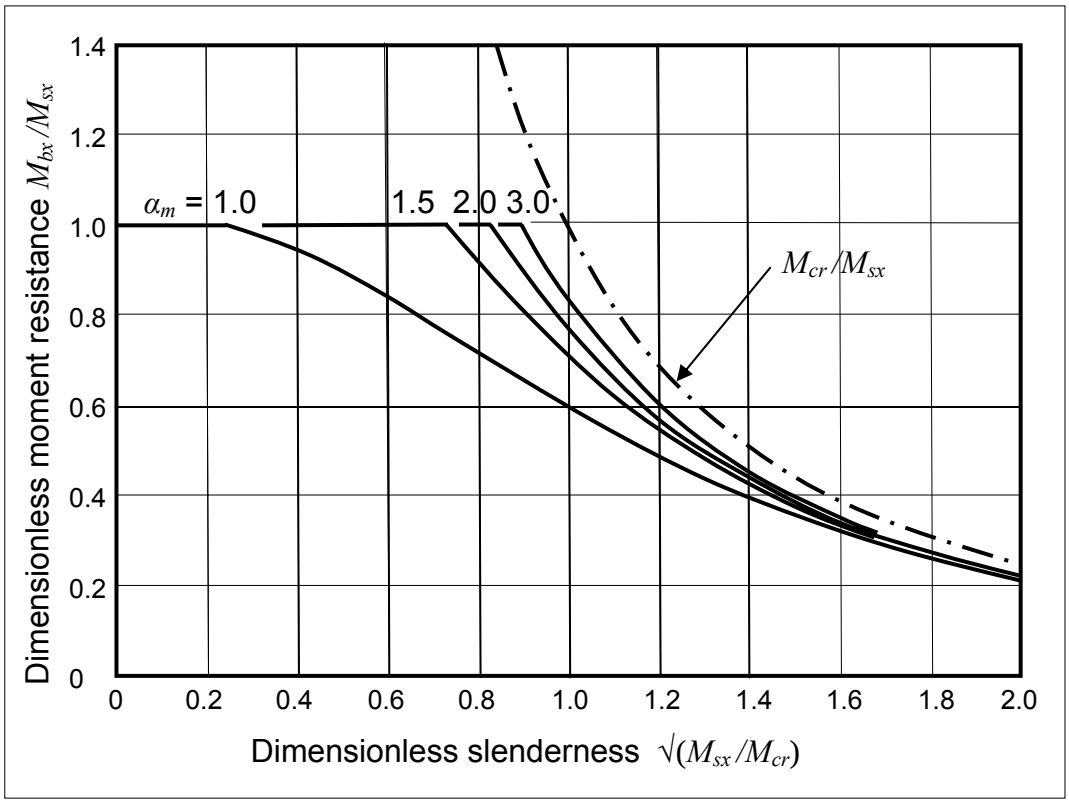

Fig. 10 Lateral buckling moment resistances of AS4100

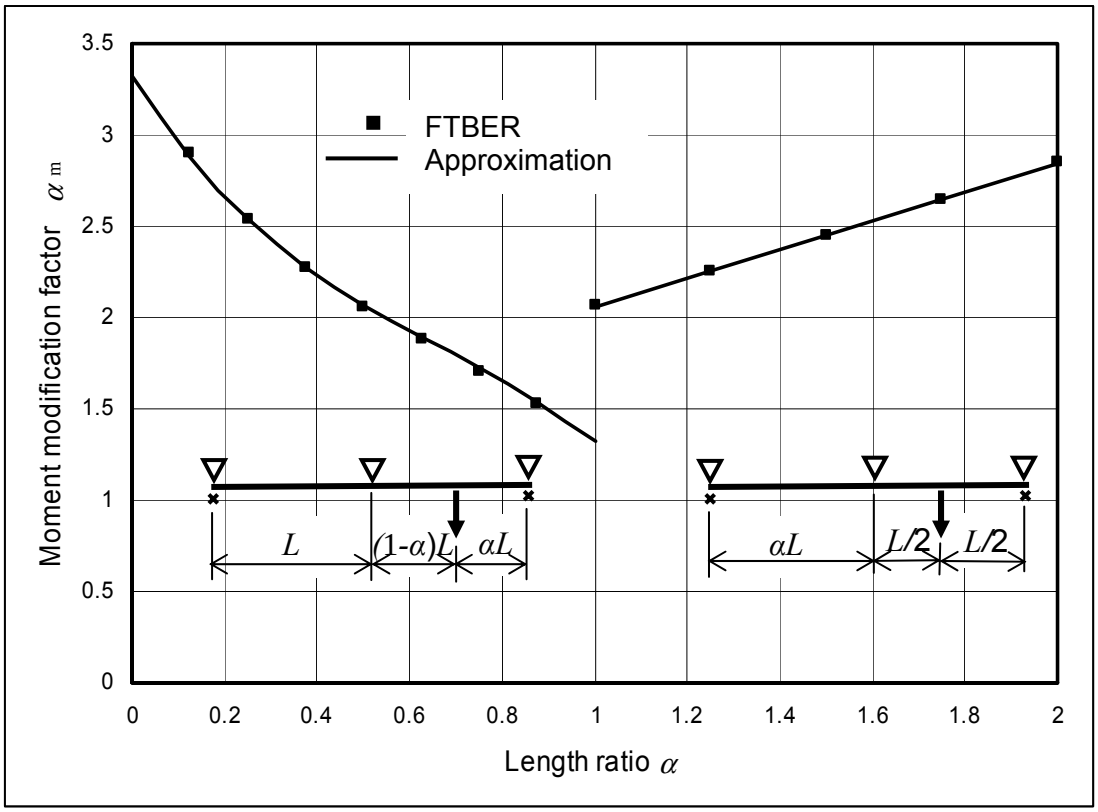

Fig. 11 Moment modification factors for two span monorails

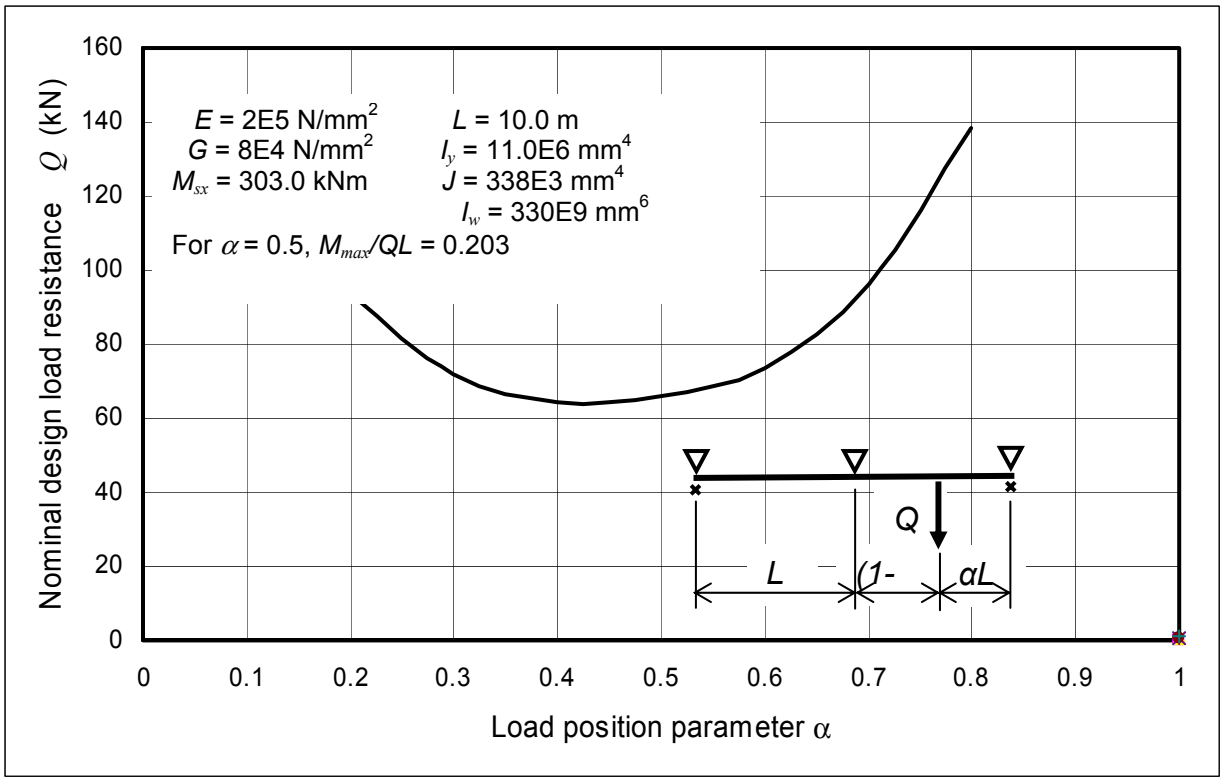

Fig. 12 Nominal design load resistances